Desalination and Water Treatment
www.deswater.com

doi: 10.5004/dwt.2018.22877

128 (2018) 414–420
October

Concentration of mine saline water in high-efficiency hybrid RO–NF system

Ewa Laskowska*, Marian Turek, Krzysztof Mitko, Piotr Dydo

Faculty of Chemistry, Department of Inorganic, Analytical Chemistry and Electrochemistry, Silesian University of Technology, B. Krzywoustego 6, 44-100 Gliwice, Poland, Tel. +48 2372103; email: Ewa.Laskowska@polsl.pl (E. Laskowska), Tel. +48 2372735; email: Marian.Turek@polsl.pl (M. Turek), Tel. +48 2371052; email: Krzysztof.Mitko@polsl.pl (K. Mitko), Tel. +48 2371052; email: Piotr.Dydo@polsl.pl (P. Dydo)

Received 27 March 2018; Accepted 10 April 2018

ABSTRACT

To obtain higher concentration of sodium chloride than in reverse osmosis (RO), the hybrid RO–nanofiltration (NF) system was applied. The use of RO retentate pressure as a driving force in NF decreased the energy consumption in the brine concentration process and increased RO permeate recovery. In such a hybrid system, NF could be regarded as an alternative method of energy recovery. Five NF membranes were tested on the synthetic sodium chloride solution, conducted at 40 bar, with highest rejection coefficients 31.3%. Selected membranes were tested at the higher pressure (50, 55 and 60 bar) on the synthetic sodium chloride solution and on the coal-mine brine RO retentate (60 bar). Based on the obtained results, energy consumption in RO–NF–vapour compression (VC) system was estimated and compared with the RO–VC system. The energy consumption in the RO–NF hybrid system with VC (123.3 kWh/m^3 of brine with 290 g/dm^3 NaCl) was lower than in the currently used RO–VC system (213.2 kWh/m^3 of brine with 290 g/dm^3 NaCl without energy recovery and 204.6 kWh/m^3 of brine with 290 g/dm^3 NaCl with energy recovery).

Keywords: Nanofiltration; Energy recovery; Saturated brine; Mine water

1. Introduction

Saturated brine (a sodium chloride solution of concentration above 300 g/dm^3) is an important resource in the chemical industry. It is usually obtained by leaching underground salt deposits or by concentration of the saline waters (seawater, water from salt lakes and mine brines) with direct thermal methods or thermal methods preceded with membrane concentration [1–7]. Saline water is increasingly often desalinated and concentrated with membrane methods: pressure-driven membrane processes (mainly reverse osmosis, RO) and electromembrane methods (electrodialysis, ED; electrodialysis reversal, EDR) [8–12]. The possibility of obtaining concentrated salt solution in RO is limited by the osmotic pressure of the feed/retentate [13,14]. In order to obtain a high permeate flux, the applied pressure must significantly exceed the osmotic pressure. In the case of seawater RO (feed osmotic pressure: ca. 26 bar), the operating pressure is 50–70 bar at the energy consumption of 2–6 kWh/m^3 of product water [15–18]. In industrial RO processes, maximum applied pressure is 80 bar, which limits the retentate salinity to about 90 g/dm^3 [19,20]. Further concentration of RO retentate may be performed by mechanical vapour compression (MVC), which typically shows the energy consumption in the range of 20–42 kWh/m^3 of feed water [18,21]. Seawater and mine water RO retentate may also be concentrated by ED/EDR (even to concentration ca. 300 g NaCl/dm^3) at the energy consumption of 7–15 kWh/m^3 of ED/EDR feedwater [18,22–25]. Coal-mine brine used in this work is currently concentrated in the 'Debiensko' Desalination Plant, where a salt crystalliser is supplied with a brine concentrated by the MVC. The energy consumption in the brine concentrator and in the brine crystalliser are 44 kWh/m^3 and 66 kWh/m^3, respectively, of distillate [26].

* Corresponding author.

Presented at the XII Scientific Conference 'Membranes and Membrane Processes in Environmental Protection' – MEMPEP 2018 13–16 June 2018, Zakopane, Poland.

1944-3994/1944-3986

Another interesting option of overcoming RO limitations resulting from high osmotic pressure of treated solution is RO–nanofiltration (NF) hybrid system. Energy consumption in RO–NF system can be decreased by 2%–12% compared with conventional multistage RO (MSRO) and water recovery can be increased from 50% (in MSRO) to 65%–85% [17,27,28]. Typical NF membranes are characterised by high rejection coefficients of multivalent ions (over 90% for SO_4^{2-}) and low rejection coefficients of monovalent ions, for example, Na^+, Cl^- (less than 60%) [29–31]. The NF permeate has a significant salinity compared with typical RO permeate; because of this, the operating pressure in NF can be much lower than in RO for the same feed: it is not the feed/retentate osmotic pressure (assuming that the RO permeate concentration value is close to zero) that should be overcome, but the difference in osmotic pressure of NF feed/retentate and NF permeate [32–34].

The aim of the research was to use a hybrid RO–NF system with vapour compression (VC) for concentration of saline waters. The RO retentate of mine water was used as a NF feed, using a pressure of the RO retentate as the driving pressure for NF. The operating pressure of NF can be much lower compared with RO for the same feed. Recirculation of the NF permeate to RO feed increases the overall permeate recovery. The proposed hybrid system produced more concentrated brine than the RO and showed higher water recovery.

2. Experimental

The NF process was carried out in the batch mode in the HP 4750 Stirred Cell Sterlitech® module of 0.3 dm^3 volume. The study was conducted on the synthetic solution of sodium chloride (60 g/dm^3) and on the RO retentate of mine water (total dissolved solids (TDS) of 56 g/dm^3). Five NF membranes – NF270 (Filmtec), NFS, NFW, NFG (Synder), Desal 5-DL (GE Osmonics) – and one tap water RO membrane – TW30 (Filmtec) were tested. The effective surface area of the membrane was 14.6 cm^2. The experiments were carried out at 40, 50, 55 and 60 bar at 20°C. Each of the membranes was conditioned with demineralised water under operating pressure and at 30% permeate recovery. In order to decrease the concentration polarization inside the module during the process, mixing with a magnetic stirrer was used. The composition of the solutions was determined by a conductometer and the ionic chromatograph (ICS-5000 Thermo Dionex, USA). The ion rejection coefficient was calculated using the following equation:

$$R = \left(1 - \frac{C_P}{C_F}\right) \times 100\% \tag{1}$$

where C_P – the ion concentration in the permeate (mg/dm^3); C_F – the ion concentration in the feed (mg/dm^3).

During the process, permeate samples were collected by every 30 cm^3 (10% of recovery) until 90% recovery was reached.

The first stage of the research involved selection of NF membranes with a sodium chloride rejection coefficient not higher than 50%. Under operating pressure of 40 bar, six membranes (five NF membranes and one RO membrane) with different rejection coefficients of sodium chloride were tested in the batch mode studies. Based on the results, the rejection coefficient and the permeate flux were calculated. The next stage was carried out with two membranes (NFS and Desal 5-DL) at three different pressures: 50, 55 and 60 bar. Based on the NaCl rejection and the permeate flux, NFS membrane was selected for further testing. The latter was carried out on NFS membrane, the applied pressure was 60 bar and the mine water RO retentate was used as a feed. Finally, based on the obtained results, energy consumption in RO–NF–VC system was estimated for different feed pressures and permeate recoveries in RO and NF and it was compared with RO–VC. For the evaporation method with VC, the energy consumption of 44 kWh/m^3 was assumed. The energy consumption of pressure-driven methods was calculated using the following equations [15,16]:

$$E = E_p + E_{\text{aux}} - E_t = \left[\frac{\text{kWh}}{\text{m}^3}\right] \tag{2}$$

$$E_p = \frac{0.02724 \times P_f}{\text{Rec} \times E_{\text{Fp}} \times F_{\text{Fm}}} = \left[\frac{\text{kWh}}{\text{m}^3}\right] \tag{3}$$

$$E_t = \frac{0.02724 \times P_c \times (1 - \text{Rec}) \times E_{\text{Ft}}}{\text{Rec} \times E_{\text{Fm}}} = \left[\frac{\text{kWh}}{\text{m}^3}\right] \tag{4}$$

where E_p – energy consumption of the high-pressure pump, E_t – energy recovered from turbines, E_{aux} – energy consumption of additional equipment, P_f – pressure at module inlet, P_c – pressure at module outlet, Rec – rate of recovery, E_{Fm} – engine efficiency, E_{Fp} – pump efficiency and E_{Ft} – turbine efficiency.

3. Results and discussion

Fig. 1 shows the relationship between the rejection coefficients of sodium chloride and the permeate recovery for the NF membranes tested at the operating pressure of 40 bar. Fig. 2 shows the relationship between the permeate flux and its recovery for all NF membranes at operating pressure of 40 bar. Table 1 shows parameters of the membranes provided by manufacturers and ones obtained in the laboratory tests.

The highest rejection coefficients of sodium chloride among the NF membranes were obtained using NFS (31.3%) and Desal 5-DL (30.5%) membranes. The drinking water RO membrane TW30 (Filmtec) was also tested, at operating pressure of 60 bar (at a lower pressure permeate flux was nearly zero) and the permeate recovery of 10%, though the permeate flux was significantly lower than in the NF process (11 $dm^3/m^2\,h$) and the sodium chloride rejection coefficient was 80%.

Further testing was carried out on two membranes (NFS and Desal 5-DL) of sodium chloride rejection coefficients closest to 50%. Tests were carried out at three different pressures: 50, 55 and 60 bar. A synthetic solution of 60 g/dm^3 of sodium chloride was used as a feed, permeate samples were taken every 30 cm^3 (10% of permeate recovery) up to 90% permeate recovery. Sample concentrations were determined

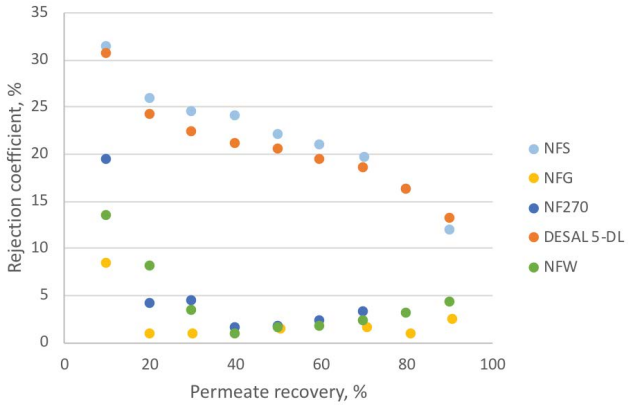

Fig. 1. Dependence of sodium chloride rejection coefficient on permeate recovery at operating pressure of 40 bar.

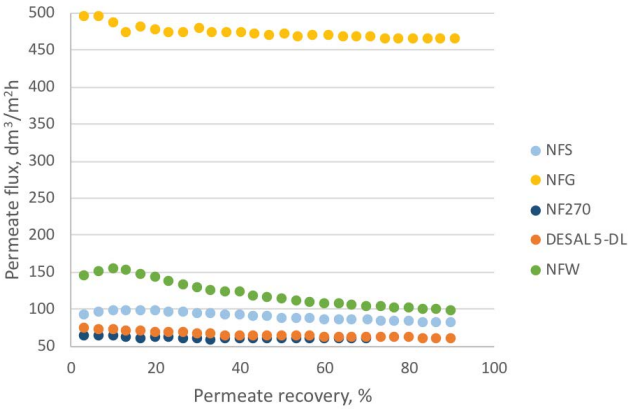

Fig. 2. Dependence of permeate flux on permeate recovery at operating pressure of 40 bar.

conductometrically. Fig. 3 shows the relationship between sodium chloride rejection coefficient and permeate recovery for NFS and Desal 5-DL membranes at operating pressures of 40, 50, 55 and 60 bar. Fig. 4 shows the relationship between permeate flux and permeate recovery for NFS and

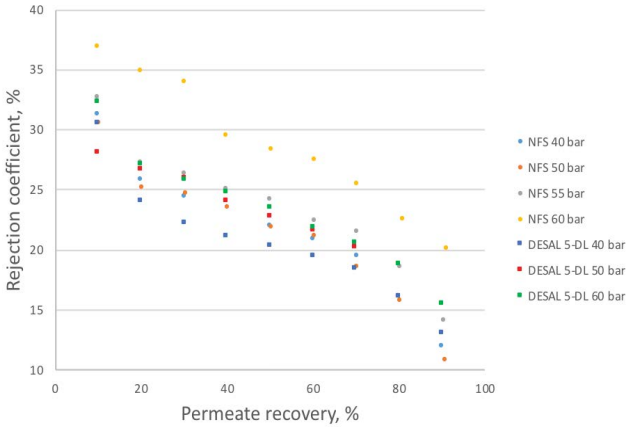

Fig. 3. Dependence of sodium chloride rejection coefficient on permeate recovery for nfs and desal 5-dL membranes.

Desal 5-DL membranes at 40, 50, 55 and 60 bar of operating pressure.

With the increase in pressure, rejection coefficients increased, and at operating pressure of 60 bar they reached 36.9% for the NFS membrane at the permeate recovery of 10% and 32.3% for the Desal 5-DL membrane at the permeate recovery of 10%. The highest permeate flux for the NFS membrane was 146.9 dm^3/m^2 h at 17% permeate recovery and it was higher than the highest permeate flux for the Desal 5-DL membrane – 98.6 dm^3/m^2 h at 23% permeate recovery.

Based on the NaCl rejection and permeate flux, the NFS membrane was selected for further tests. NF was carried out at a pressure of 60 bar. The RO retentate of mine water was used as a NF feed. Permeate samples were taken every 50 cm^3 (16.67% of permeate recovery) until 50% permeate recovery was reached. Concentrations of the most important ions, Cl^-, SO_4^{2-}, Na^+, Ca^{2+} and Mg^{2+}, were determined using an ion chromatograph. Table 2 shows the obtained rejection coefficients for individual ions depending on the permeate recovery.

Fig. 5 shows the dependence of permeate flux on permeate recovery and on the feed water type (the retentate of the

Table 1
Rejection coefficients of sodium chloride and magnesium sulphate as provided by the manufacturers and obtained in the laboratory tests

Membrane	MWCO (Da)	Minimum $MgSO_4$ rejection coefficients declared by the manufacturer (%)	NaCl rejection coefficients declared by the manufacturer (%)	Maximum NaCl rejection coefficients obtained in laboratory tests (%)[3]
NFS	100–250	99.5*	50–55[1]	31.3
NFW	300–500	97.0*	20.0[1]	13.4
NFG	600–800	50.0*	10.0[1]	8.3
NF270	200–400	97***	50[2]	19.4
Desal 5-DL	150–300	96**	No data	30.5

*Test: 2,000 ppm $MgSO_4$, operating pressure 760 kPa and temperature: 25°C.
**Test: 5,000 mg/dm^3 $MgSO_4$, operating pressure 655 kPa, recovery 15% and temperature: 25°C.
***Test: 2,000 ppm $MgSO_4$, operating pressure 4.8 bar, recovery 15% and temperature: 25°C.
[1]Test: 2,000 ppm NaCl, operating pressure 760 kPa and temperature: 25°C.
[2]Test: 2,000 mg/dm^3 NaCl, operating pressure 3.5 bar and temperature 25°C.
[3]Test: 60 g/dm^3 NaCl, operating pressure 40 bar and temperature 20°C.

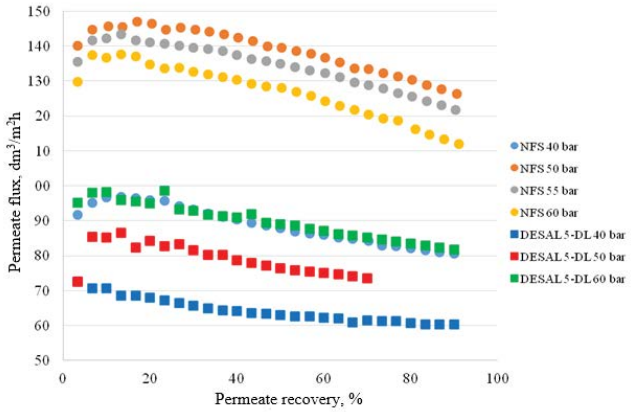

Fig. 4. Dependence of permeate flux on permeate recovery for nfs and desal 5-dL membranes.

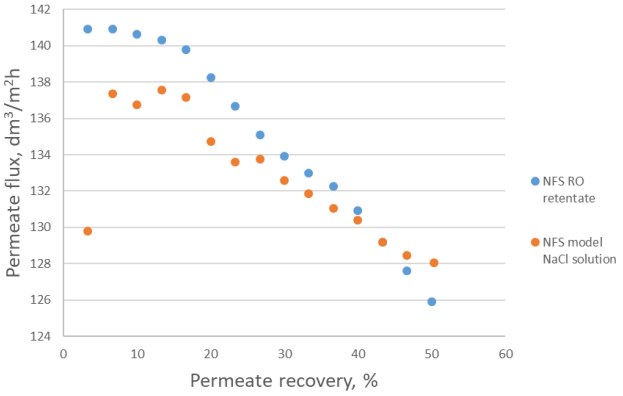

Fig. 5. Dependence of nfs membrane permeate flux on permeate recovery and on feed type.

Table 2
Results of nanofiltration using reverse osmosis retentate as feed on NFS membrane

Permeate	Permeate recovery (%)	R_{Cl^-} (%)	$R_{SO_4^{2-}}$ (%)	R_{Na^+} (%)	$R_{Mg^{2+}}$ (%)	$R_{Ca^{2+}}$ (%)
P1	16.67	26.9	94.9	22.7	62.5	36.6
P2	33.33	39.9	95.4	36.3	70.5	49.2
P3	50.00	42.6	95.5	39.3	70.1	49.8

RO of the mine brine and the NaCl synthetic solution) using the NFS membrane. The permeate flux was higher when RO retentate was used as a feed.

Based on the obtained results, the energy consumption in RO–NF–VC system was estimated for different feed pressures and permeate recoveries in RO and NF. In addition, the energy consumption of brine concentration systems (concentration of Cl^- 176 g/dm³): RO–VC and RO–NF–VC was compared.

For the calculation of the energy consumption in RO, the following values were used: feed TDS 30 g/dm³, recovery 35%–50%, ionic rejection coefficient above 99%, operating pressure 55–64 bar. In the calculation of the energy consumption in NF, as a feed TDS of RO retentate was used at recovery 35%–50%, in the case of too low RO retentate pressure, booster pump was applied to expected pressure: 54–68 bar. The energy consumption in RO–VC system was calculated for two cases with and without energy recovery and for RO–NF–VC system only without energy recovery. Table 3 summarises energy consumption values for the processes.

Figs. 6 and 7 show the obtained results of the energy consumption, composition and permeate recovery in RO–VC and RO–NF–VC systems using NFS membrane in NF.

Desalinated water and brine are products in RO–NF–VC system. In refer to Ahunbay et al. [17] RO–NF system, which achieved 2.3–2.8 kWh/m³ of water, calculated energy consumption in RO–NF system (Table 3) was 2.8–3.3 kWh/m³ of water and 14.4–22.5 kWh/m³ of water in RO–NF–VC system.

Table 3
Energy consumption values for RO–NF–VC and RO–NF with different feed pressures and permeate recoveries in RO and NF

RO recovery (%)	Pressure (bar)			NF recovery (%)	Energy consumption in RO–NF–VC (kWh/m³ of brine)	Energy consumption in RO–NF–VC (kWh/m³ of water)	Energy consumption in RO–NF (kWh/m³ of water)
	RO feed	RO retentate	NF feed				
35	55.79	53.79	54.33	45	191.8	22.50	3.1
35	55.66	53.66	55.81	50	183.2	21.49	3.3
40	58.24	56.24	56.55	40	177.9	20.87	2.9
40	57.91	55.91	57.89	45	170.2	19.97	3.1
40	57.87	55.87	58.59	50	161.7	18.97	3.3
45	60.7	58.7	60.43	40	157.5	18.48	2.9
45	60.43	58.43	62.1	45	150.0	17.60	3.1
45	60.48	58.48	63.07	50	141.7	16.62	3.3
50	64.08	62.08	62.1	35	145.0	17.01	2.8
50	63.64	61.64	65.07	40	138.3	16.23	3.0
50	63.44	61.44	67.14	45	131.1	15.38	3.1
50	63.61	61.61	68.43	50	123.4	14.48	3.3

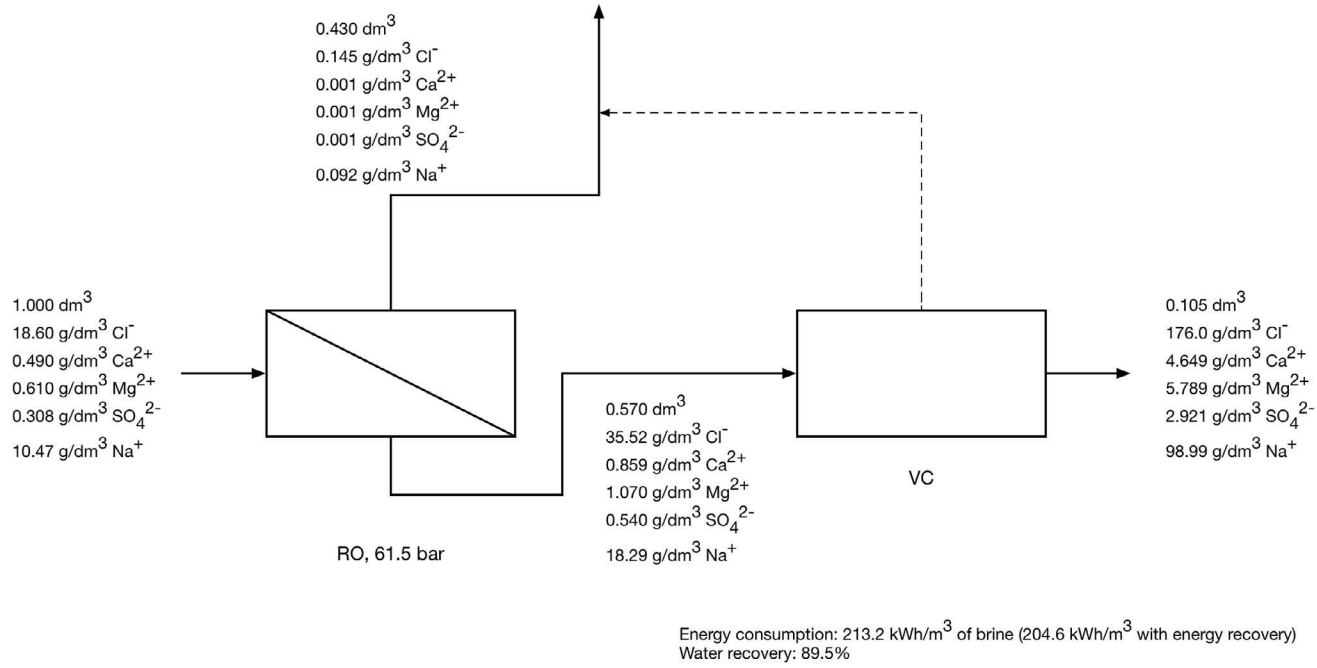

Fig. 6. The block diagram of brine concentration process by RO - VC method.

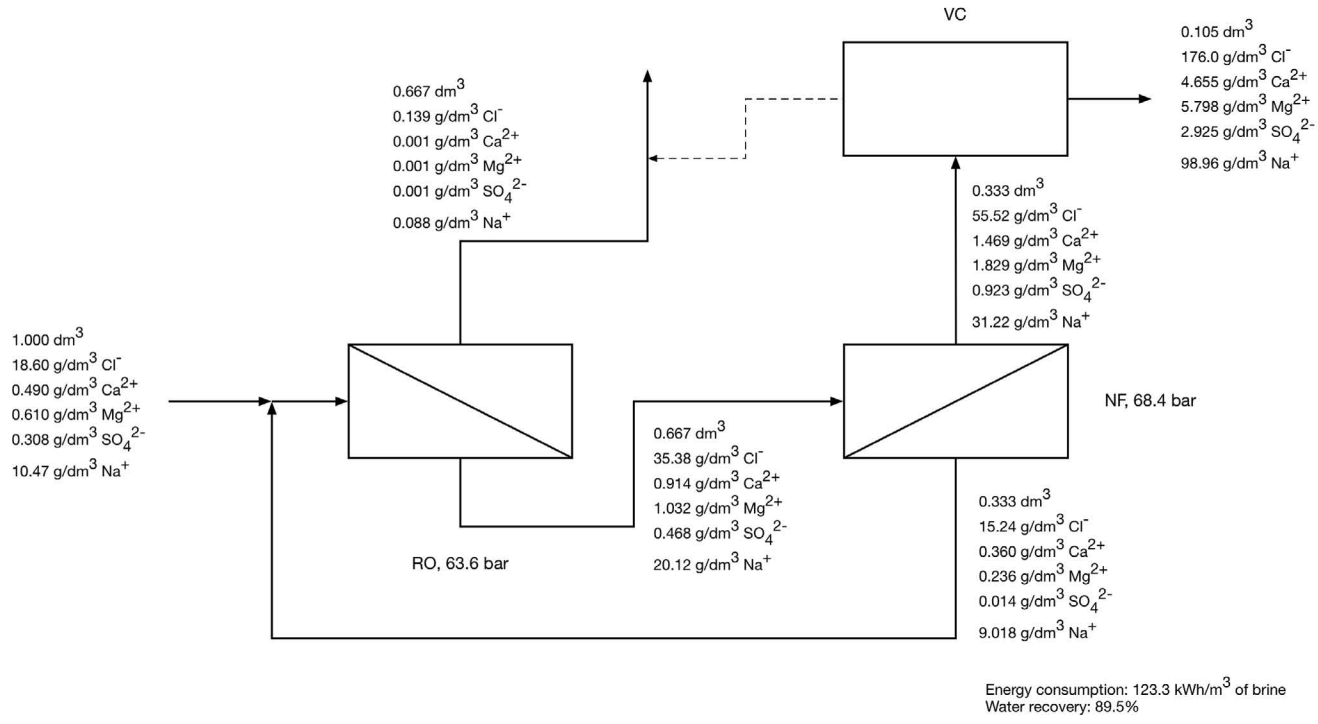

Fig. 7. The block diagram of brine concentration process by RO – NF – VC method.

Chong et al. [27] considered a multistage energy-efficient RO, using first- and third-stage retentate pressure as a feed pressure to second stage, with energy consumption 2.3–3.5 kWh/m^3 of water. Turek et al. [35] considered a hybrid NF–RO–ED system to produce desalinated water and brine (TDS 300 g/dm^3), with the energy consumption 6.9 kWh/m^3 of water and 79.35 kWh/m^3 of brine. Macedonio et al. [36] proposed an integrated microfiltration–NF–RO system with a membrane crystallization on NF retentate and a membrane distillation on RO retentate for simultaneous production of desalinated water and brine (TDS 240 g/dm^3), with the energy consumption 27.52–28.00 kWh/m^3 of water

(1.61–2.05 kWh/m^3 of water if thermal energy or the stream is available in the plant) and 216.56–220.10 kWh/m^3 of brine (12.65–16.12 kWh/m^3 of brine if thermal energy or the stream is available in the plant).

4. Conclusions

During the experiments on the synthetic sodium chloride solutions, conducted at 40 bar, the highest rejection coefficients were observed for NFS (31.3%) and DESAL (30.5%) NF membranes. The remaining NF membranes had lower rejection coefficients, down to NFG showing almost negative ones. The RO membrane, TW30 (Filmtec), was tested at 60 bar – despite 80% rejection coefficient, the permeate flux was lower by one order of magnitude compared with NF membranes. The NFS membrane showed higher permeate flux than the DESAL membrane and it was tested using real solution – RO retentate from a coal mine desalination plant. Based on the ion rejection coefficients obtained in the bench-scale testing of NF using NFS membrane, a hybrid RO–NF–VC system was designed and compared with RO–VC system. The proposed hybrid RO–NF–VC system showed lower energy consumption than the existing RO–VC system (123.3 vs 204.6 kWh/m^3 of brine, respectively) at the same overall water recovery. In the proposed system, NF could be treated as an alternative energy recovery device for RO.

Symbols

R — Ion rejection coefficient, %
C_P — Ion concentration in permeate, mg/dm^3
C_F — Ion concentration in feed, mg/dm^3
E_p — Energy consumption of the high-pressure pump, kWh/m^3
E_t — Energy recovered from turbines, kWh/m^3
E_{aux} — Energy consumption of additional equipment, kWh/m^3
P_f — Pressure at module inlet, bar
P_c — Pressure at module outlet, bar
Rec — Rate of recovery, recovery, %
E_{Fm} — Engine efficiency, kWh/m^3
E_{Fp} — Pump efficiency, kWh/m^3
E_{Ft} — Turbine efficiency, kWh/m^3

Acknowledgment

This work was financed by the Polish National Science Centre upon Decision No. DEC-2014/13/B/ST8/04263.

References

[1] F.J. Arias, Deliberate salinization of seawater for desalination of seawater, J. Energy Resour. Technol., 140 (2018) 032004-1–032004-5.
[2] Y. Shen, T. Wang, NaCl brine preparation from distiller waste and Na_2SO_4, Adv. Mater. Res., 233–235 (2011) 897–902.
[3] Y.V. Pinneker, Fully saturated brines, Int. Geol. Rev., 10 (1968) 603–607.
[4] L.M. Vane, Water recovery from brines and salt-saturated solutions: operability and thermodynamic efficiency considerations for desalination technologies, J. Chem. Technol. Biotechnol., 92 (2017) 2506–2518.
[5] P. Marchand, Production of sea salt, Ind. Mineral. Min. Carrieres, 68 (1986) 529–534.
[6] P. Pierzyna, M. Popczyk, T. Suponik, Testing the possibility of leaching salt debris obtained from underground excavations, E3S Web Conf., 18 (2017) Article number 01033.
[7] H.W. Chung, K.G. Nayar, J. Swaminathan, K.M. Chehayeb, J.H. Lienhard, Thermodynamic analysis of brine management methods: zero-discharge desalination and salinity-gradient power production, Desalination, 404 (2017) 291–303.
[8] M.K. Wittholz, B.K. O'Neill, C.B. Colby, D. Lewis, Estimating the cost of desalination plants using a cost database, Desalination, 229 (2008) 10–20.
[9] B.A. Qureshi, S.M. Zubair, Exergetic efficiency of NF, RO and EDR desalination plants, Desalination, 378 (2016) 92–99.
[10] M.S. Osman, J.J. Schoeman, L.M. Baratta, Desalination/concentration of reverse osmosis and electrodialysis brines with membrane distillation, Desal. Wat. Treat., 24 (2010) 293–301.
[11] R. Bórquez, J. Ferrer, Seawater desalination by combined nanofiltration and ionic exchange, Desal. Wat. Treat., 57 (2016) 28122–28132.
[12] M. Turek, M. Gonet, Nanofiltration in the utilization of coal-mine brines, Desalination, 108 (1997) 171–177.
[13] B.K. Pramanik, L. Shu, V. Jegatheesan, A review of the management and treatment of brine solutions, Environ. Sci. Water Res. Technol., 3 (2017) 625–658.
[14] C.A. Quist-Jensen, F. Macedonio, E. Drioli, Membrane crystallization for salts recovery from brine—an experimental and theoretical analysis, Desal. Wat. Treat., 57 (2016) 7593–7603.
[15] P. Brewer, The key to efficient RO desalination, Filtr. Sep., 53 (2016) 20–22.
[16] M. Wilf, Fundamentals of RO-NF Technology, International Conference on Desalination Costing, Cyprus, 2004, pp. 18–31.
[17] M. Göktuğ Ahunbay, S. Birgül Tantekin-Ersolmaz, W.B. Krantz, Energy optimization of a multistage reverse osmosis process for seawater desalination, Desalination, 429 (2018) 1–11.
[18] T. Tong, M. Elimelech, The global rise of zero liquid discharge for wastewater management: drivers, technologies, and future directions, Environ. Sci. Technol., 50 (2016) 6846–6855.
[19] L.F. Greenlee, D.F. Lawler, B.D. Freeman, B. Marrot, P. Moulin, Reverse osmosis desalination: water sources, technology, and today's challenges, Water Res., 43 (2009) 2317–2348.
[20] Y. Kunisada, H. Kaneda, M. Hirai, Y. Murayama, Seawater desalination by reverse osmosis in Chigasaki laboratory, Coating Conference, Proc. Technical Association of the Pulp and Paper Industry, 2017, pp. 337–345.
[21] R. Schwantes, K. Chavan, D. Winter, C. Felsmann, J. Pfafferott, Techno-economic comparison of membrane distillation and MVC in a zero liquid discharge application, Desalination, 428 (2018) 50–68.
[22] Y. Tanaka, R. Ehara, S. Itoi, T. Goto, Ion-exchange membrane electrodialytic salt production using brine discharged from a reverse osmosis seawater desalination plant, J. Membr. Sci., 222 (2003) 71–86.
[23] M. Reig, S. Casas, C. Aladjem, C. Valderrama, O. Gilbert, F. Valero, C.M. Centeno, E. Larrotcha, J.L. Cortina, Concentration of NaCl from seawater reverse osmosis brines for the chlor-alkali industry by electrodialysis, Desalination, 342 (2014) 107–117.
[24] M. Turek, K. Mitko, M. Chorążewska, P. Dydo, Use of the desalination brines in the saturation of membrane electrolysis feed, Desal. Wat. Treat., 51 (2013) 2749–2754.
[25] C. Jiang, Y. Wang, Z. Zhang, T. Xu, Electrodialysis of concentrated brine from RO plant to produce coarse salt and freshwater, J. Membr. Sci., 450 (2014) 323–330.
[26] M. Turek, P. Dydo, R. Klimek, Salt production from coal-mine brine in ED–evaporation–crystallization system, Desalination, 184 (2005) 439–446.
[27] T.H. Chong, S.L. Loo, W.B. Krantz, Energy-efficient reverse osmosis desalination process, J. Membr. Sci., 473 (2015) 177–188.
[28] J.R. Herron, E. Beaudry, K.A. Lampi, Method and System for Generating Strong Brines, Hydration Systems, LLC, US20150014248 A1, 2015.
[29] V. Preuß, C. Riedel, T. Koch, K. Thűrmer, M. Domańska, Nanofiltration as an effective tool of reducing sulphate concentration in mine water, Archit. Civil Eng. Environ., 3 (2012) 127–132.

[30] M. Nyström, L. Kaipia, S. Luque, Fouling and retention of nanofiltration membranes, J. Membr. Sci., 98 (1995) 249–262.
[31] A.I. Schäfer, A.G. Fane, T.D. Waite, Nanofiltration - Principles and Applications, Elsevier, Oxford, UK; New York, NY, 2005.
[32] L. Llenas, X. Martínez-Lladó, A. Yaroshchuk, M. Rovira, J. de Pablo, Nanofiltration as pretreatment for scale prevention in seawater reverse osmosis desalination, Desal. Wat. Treat., 36 (2011) 310–318.
[33] D. Zhou, L. Zhu, Y. Fu, M. Zhu, L. Xue, Development of lower cost seawater desalination processes using nanofiltration technologies — a review, Desalination, 376 (2015) 109–116.
[34] J. Liu, J. Yuan, L. Xie, Z. Ji, Exergy analysis of dual-stage nanofiltration seawater desalination, Energy, 62 (2013) 248–254.
[35] M. Turek, K. Mitko, E. Laskowska, M. Chorążewska, K. Piotrowski, A. Jakóbik-Kolon, P. Dydo, Energy consumption and gypsum scaling assessment in a hybrid nanofiltration-reverse osmosis-electrodialysis system, Chem. Eng. Technol., 41 (2018) 392–400.
[36] F. Macedonio, E. Curcio, E. Drioli, Integrated membrane systems for seawater desalination: energetic and exergetic analysis, economic evaluation, experimental study, Desalination, 203 (2007) 260–276.